Nuclear Instruments and Methods in Physics Research A 619 (2010) 401–407

Contents lists available at ScienceDirect

Nuclear Instruments and Methods in Physics Research A

journal homepage: www.elsevier.com/locate/nima

Convenient fabrication of three-dimensional cell-culture substrates through introduction of micrometer-size pores on polyallyldiglycol carbonate polymer films

C.K.M. Ng [a], J.P. Cheng [b], S.H. Cheng [b], K.N. Yu [a,*]

[a] Department of Physics and Materials Science, City University of Hong Kong, Hong Kong
[b] Department of Biology and Chemistry, City University of Hong Kong, Hong Kong

ARTICLE INFO

Available online 25 October 2009

Keywords:
Solid-state nuclear track detector
SSNTD
Alpha particle
PADC
Three-dimensional substrate

ABSTRACT

We explored the fabrication of three-dimensional (3D) substrates by creating micrometer-size pores on polyallyldiglycol carbonate (or PADC) polymer films through irradiation of the film by alpha particles and subsequent chemical etching. HeLa cells cultured on these 3D substrates were observed using scanning electron microscope. Multiple directions and multiple layers of HeLa cells were observed to have grown in the pores, with normal nuclei and cell membranes as well as good cell spreading. For the cells cultured in 3D substrates with or without additional small pores, no significant differences were observed between their vinculin expression profiles, which were in contrast to the observation made for cells cultured on 2D substrates showing that small pores could enhance vinculin expression. The presence of the large pores and/or the enhanced biocompatibility of the substrate in the present experiments might be the reasons. The protrusions of cells were confined by the small pores, which was similar to the observation made for cells cultured on 2D substrates.

1. Introduction

In vitro experiments rely heavily on tissue culture, e.g., to study the cell differentiation, proliferation, function, etc. These *in vitro* experiments usually involve flat culture substrates, e.g., through the use of Petri dishes and flasks, and are thus convenient for routine growth of cells. However, such conventional cell culture will normally generate only two-dimensional (2D) cell monolayers. Such 2D monolayers will lead to highly abnormal geometric and mechanical pressures on many types of cells, which are far from the realistic conditions and complexities of three-dimensional (3D) tissues [1].

It is well established that cells in tissues connect to each other and to the extra-cellular matrix (ECM). Receptor complexes on the surface of cells facilitate interactions with their neighbors, with the ECM and other exogenous factors, to enable cells to interpret the multitude of physical and biochemical cues from the immediate environment. Moreover, 3D mammalian cell culture promotes normal epithelial polarity and differentiation [1]. Considering this intricate mechanical and biochemical interplay, important biological properties may be missed if the cells are studied within a 2D culture system. The lack of dorsal anchorage points in 2D cultures affects the balance between cell spreading or retracting, creating an unnatural stimulatory environment for the organization of lamellipodia, stress fibers and focal adhesions. This imbalance leads the cells to spread out in an extreme manner. It has been found that the context in which a cell is grown matters and changing the environment can radically alter the behavior of cells [2]. In relation, there have been many studies on the advantages of 3D cell culture environment when compared to the 2D case. Cells have been shown to move and divide more quickly, and to have a characteristically asymmetric shape as those in living tissues [3]. The spatial arrangement of ECM receptors in 2D is mainly concentrated on the ventral surface, whereas in 3D cultures they are spread over the entire surface.

Evidences have suggested that modification of cell growth conditions can radically affect the behavior of cells in response to chemical reagents [4]. In addition, researches have shown that cancerous breast cells growing in 3D have patterns of gene expression and other biological activities that more closely reflect the activities of cells in living tissues [5,6]. There is also a substantial amount of evidence that cells growing in 3D are more resistant to cytotoxic agents than cells grown in monolayer or in a dispersed culture [7]. Studies have demonstrated an elevated level of drug resistance of spheroids culture compared with cells in monolayer [7]. Initially, investigators attributed the drug resistance of spheroids to poor diffusion of the drugs to interior cells but now it has been proved that the 3D culture itself accounts for

* Corresponding author. Tel.: +852 2788 7812; fax: +852 2788 7830.
E-mail address: peter.yu@cityu.edu.hk (K.N. Yu).

0168-9002/$ - see front matter © 2009 Elsevier B.V. All rights reserved.
doi:10.1016/j.nima.2009.10.122

drug resistance [8,9]. Furthermore, culturing human pluripotent stem cells on 3D scaffolds can markedly affect the cell behavior [10,11] by offering growing tissues the opportunity to exploit additional space and form alternative interactions with neighboring cells, noting that interactions are restricted in cultures grown as 2D monolayer.

As such, *in vitro* experiments involving 2D cell monolayer will inevitably suffer from the limitation that they do not adequately represent the functions of 3D tissues, and the relevance of results from *in vitro* experiments to *in vivo* animal or human studies is thus continually challenged. Accordingly, it has always been desirable to design and fabricate convenient and economical substrates which can allow the cells to grow in a 3D manner, so as to mimic functions and responses of cells in real tissues. For examples, 3D cell cultures have been used extensively recently, particularly in tissue engineering applications, e.g., cell-seeded scaffolds [12] and patterned cocultures [13] as well as in directing cell fate and differentiation [14], to mimic native micro-environments. This is a crucial step for improving the predictive accuracy or in understanding cell metabolism and other cell behaviors [15,16].

In the present work, we have explored the fabrication of such a 3D substrate by creating micrometer-size pores on polyallyldiglycol carbonate (or PADC) polymer films through irradiation of the film by alpha particles and subsequent chemical etching. PADC film is one commonly used solid-state nuclear track detector (SSNTD). There was a recent review on SSNTDs and their applications [17]. PADC is sometimes commercially available under the name CR-39, which is widely used in different branches of sciences. In particular, as they can record alpha particles, thin PADC films with a thickness of 10–20 μm have been proposed as cell-culture substrates for alpha-particle radiobiological experiments (e.g., [18–20]). Previous experiments have been performed to study the topographic effect on cell behavior (e.g., [21]). In particular, it has been established that changes in the surface topography of SSNTDs through chemical etching or superficial pore formation can enhance the biocompatibility [22,23].

2. Methodology

2.1. Characterization of PADC films

In the present work, "thick" PADC films with a thickness of 1000 μm from Page Mouldings (Pershore) Limited, Worcestershire were employed. Although in reality we will use "thin" PADC films with a thickness of 10–20 μm, the physical and chemical properties of thick and thin PADC films are the same, with the thick films being more convenient to handle.

PADC films with a size of $2 \times 2\,cm^2$ have been prepared as substrates for cell cultivation. In the present experiments, there were two types of treated PADC films. Both types of treated films were irradiated with 5 MeV alpha particles using an ^{241}Am alpha-particle source and were then subsequently chemically etched by 6.25 N aqueous NaOH at 70 °C for 30 h, which is the most commonly employed conditions, giving a bulk etch rate of ~1.2 μm/h [24].

One type of treated films was etched for 30 h. The other type of treated films were first etched for 27 h, then irradiated by 3 MeV alpha particles for 6 h (with an average track density of about 830,000 tracks cm^{-2}), and subsequently further etched for 3 h, so the aggregate etching time was also 30 h. As a final step, both types of treated (and etched) PADC films were further etched for 5 min in 1 N NaOH/ethanol at 40 °C (with a bulk etch rate of ~9.5 μm/h [25]). The PADC films were etched in NaOH/ethanol in the end because Li et al. [18] found that this step would bring about better biocompatibility.

Upon the chemical etching steps, the 5 MeV alpha-particle irradiation with 30 h etching will lead to larger pores while the 3 MeV alpha-particle irradiation with 3 h etching will lead to smaller pores. The dimensions of large pores and small pores were measured experimentally. Those for the large pores were determined using a surface profilometer (Form Talysurf PGI Profilometer, Taylor Hobson, England), which was a contact stylus instrument based on a phase grating interferometric (PGI) transducer. During measurements, a computer-controlled stylus scanned slowly across a surface of the specimen. The movement of the stylus was converted into an electrical signal by the computer and the profile of the scanned surface was generated. The small pores were tracks in the sharp phase, which was described in a previous paper [23]. For a comparison, the opening diameters of pores in PADC films formed by etching in $NaOH/H_2O$ alone were calculated using the computer program called TRACK_TEST [17] (also freely available on the webpage: http://www.cityu.edu.hk/ap/nru/test.htm). It is remarked here that the opening diameters can no longer be simulated using TRACK_TEST after a further etching in NaOH/ethanol for 5 min, since the *V* function (ratio between the track etch rate and the bulk etch rate) of PADC in NaOH/ethanol, which is required by the TRACK_TEST program for computation, is unknown. On the other hand, the dimensions for the small pores were determined from their lateral images after polishing the edge of the films as described in a previous paper [23].

2.2. Cell culture

HeLa cervix cancer cells were obtained from the American Type Culture Collection. HeLa cells were cultured on the $2 \times 2\,cm^2$ PADC films with different treatments as described in Section 2.1. Before cell culture, the PADC films were sterilized by submerging in 75% (v/v) ethyl alcohol for 2 h and then immersed in fresh medium for 24 h before cell culture. These films were then used for HeLa cell culture. HeLa cells were maintained as exponentially growing monolayer at low-passage numbers in Dulbecco's modified eagle medium (D-MEM) supplemented with 10% fetal bovine serum, 1% (v/v) penicillin/streptomycin (Gibco, Germany). The cells were cultured at 37 °C in humidified atmosphere containing 5% CO_2. Sub-cultivation was performed every 3–4 d. The cells were trypsinized with 0.5%/0.2% (v/v) trypsin/EDTA (ethylenediamine-tetra-acetic acid; Gibco), adjusted to 4.5×10^5 cells in 3 ml medium and plated out on the PADC films placed inside a 35 mm diameter Petri dish. All cells were allowed to plate out on the PADC films for 1 d.

2.3. Scanning electron microscope observation

Scanning electron microscope (SEM) was used in order to have a better view of cells seeded on large pores. Substrates with large pores were immersed in 0.1 mg/ml polylysine in MilliQ before cell seeding to improve cell adherence. The cells cultured on PADC films with different treatments were fixed in fixation buffer (2% paraformaldehyde, 2.5% Gluta, 0.1 M cacodylate buffer, pH 7.2, 0.05% $CaCl_2$) overnight at RT for 2 h. The fixed cells were washed with washing buffer (0.1 M cacodylate buffer (pH 7.2)) for 5–10 min five times at RT. Then, the cells were post-fixed with 2% OsO_4 in 0.1 M cacodylate buffer (pH 7.2) at RT for 2 h. The post-fixed cells were transferred from the washing buffer into the water and then dehydrated gradually with ethanol. After dehydration, cells were gradually transferred to acetone at RT and then critical-point-dried in liquid CO_2. The dried PADC films were mounted, with cells at the surface top, on aluminum stubs with double side carbon tape (Nisshin EM Co. Ltd., Tokyo) and then gold-coated by using a sputter coater. The samples were then

examined and photographed with a SEM (Philips XL30 ESEM-FEG) operating at 10 kV and a magnification of 1500 ×.

2.4. Immunohistochemical localization studies

Immunohistochemical localization studies were carried out to study the expression of vinculin. Rhodamine–phalloidin was used to label F-actin and Hoechest 33342 was applied for nucleus staining. Briefly, the cells cultured on PADC films with different treatments were fixed with 4% formaldehyde solution in PBS for 10 min at room temperature. After washing two or more times with PBS, they were extracted with PBS supplied with 0.5% Triton X-100 for 5 min. Nonspecific binding was blocked with 5% goat serum in PBS for 30 min. Subsequently, the samples were incubated for 1 h with a mouse monoclonal antibody (mAB) to human vinculin (MAB1674, Chemicon International, CA; diluted 1:50 in PBS containing 5% normal goat serum and 0.05% Tween20). The samples were washed two times with PBS and followed by Alexa 488 anti-mouse IgG (Molecular Probes, A11029) secondary antibody (diluted 1:100 in PBS containing 5% normal goat serum and 0.05% Tween20) for 30–45 min. The samples were washed with PBS and then incubated for 15 min with 80 μg/ml Rhodamine–phalloidin (diluted in PBS containing 0.05% Tween20 and 1% BSA). Subsequently, they were washed two times or more with PBS and incubated with 1 μg/ml Hoechest 33342 in PBS for 7 min. The samples were washed two times with PBS before imaging under a confocal laser scanning microscope (Leica TCS SPE) with 63 × objectives.

3. Results

3.1. Topography of alpha-particle irradiated and chemically etched PADC films

By using the program TRACK_TEST, the dimensions of the large pores were determined as: diameter $2r=43.9\,\mu m$, depth $d=15.4\,\mu m$ and aspect ratio $d/2r=0.351$.

Experimentally, the dimensions of the large pores after etching in $NaOH/H_2O$ and then in NaOH/ethanol were determined by Form Talysurf PGI Profilometer. The 3D profile obtained for a pore is shown in Fig. 1(a)–(c). The opening diameter $2r$ and depth d were increased to 50.7 ± 0.4 and $18.8\pm0.2\,\mu m$, respectively (aspect ratio $d/2r$ changed to 0.371 ± 0.005, which was also slightly increased), after etching in NaOH/ethanol.

The pores are in the spherical phase as shown in Fig. 1. A pore in the spherical phase is in fact represented by a part of a sphere, so that the radius of the pore opening r is related to the radius of the sphere R through

$$r=\sqrt{R^2-(R-d)^2}. \quad (1)$$

The volume of the pore is given by

$$V=\pi\left(Rd^2-\frac{d^3}{3}\right) \quad (2)$$

and the area of the curved surface of the pore is given by

$$A=2\pi Rd. \quad (3)$$

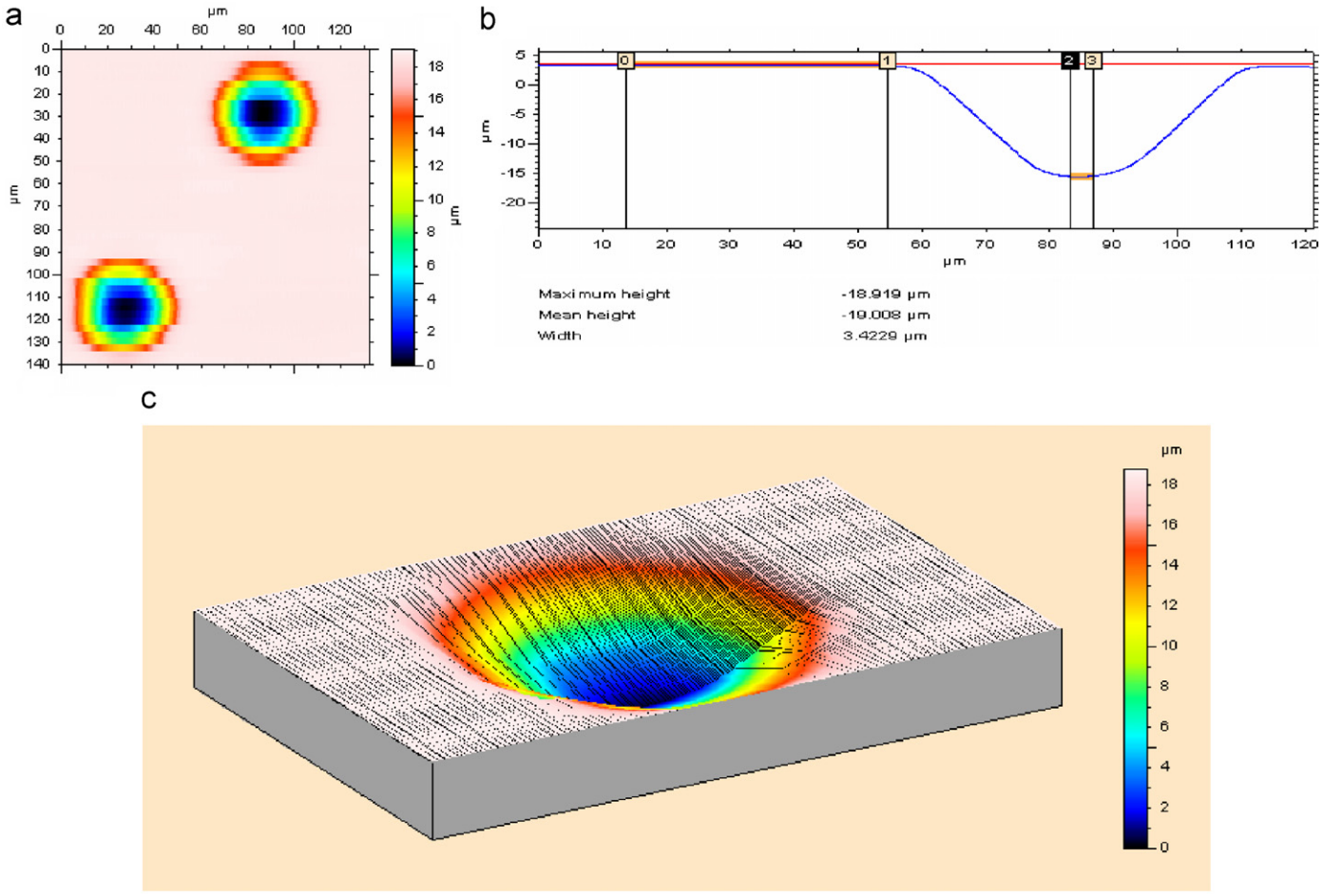

Fig. 1. The profile of a large pore in a PADC film generated by a normally incident 5 MeV alpha particle and subsequent chemical etching for 30 h recorded using a surface profilometer. (a) Top view; (b) cross-sectional view; (c) 3D view.

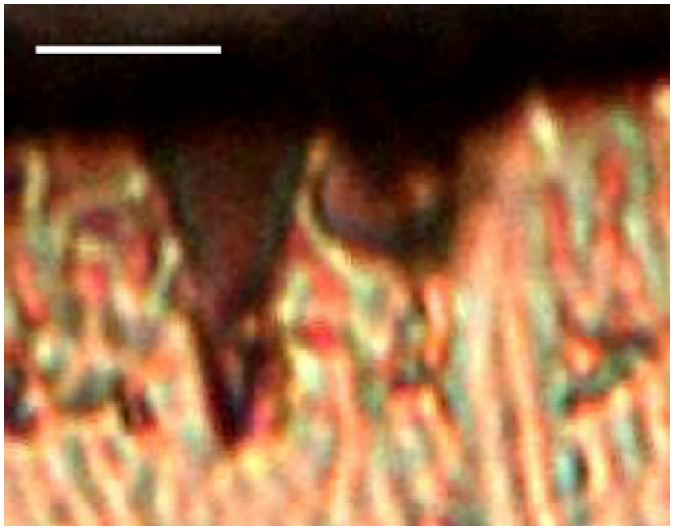

Fig. 2. The lateral view of a conical pore generated from an alpha particle with incident energy of 3 MeV (etched for 3 h in 6.25 N aqueous NaOH at 70 °C and then for 5 min in 1 N NaOH/ethanol at 40 °C) revealed under the optical microscope operated in the transmission mode after polishing the edge of the film. Bar=5 μm [23].

The radius of the pore opening was measured as $r=25.4\pm0.2\,\mu m$, so the radius R of the sphere was $26.5\pm0.42\,\mu m$ using Eq. (1). The volume V and the surface area A of the pore were determined as $22400\pm300\,\mu m^3$ and $3000\pm60\,\mu m^2$.

The dimensions of the small pores were also measured experimentally from their lateral views under the optical microscope, after cleaving the PADC films in directions perpendicular to the pore openings and after polishing the cleavage surfaces. Fig. 2 shows the lateral view of a conical pore revealed under the optical microscope operated in the transmission mode. The opening diameter and depth of the small pores after etching in $NaOH/H_2O$ and then in NaOH/ethanol were determined [23] as 4.8 ± 0.1 and $6.6\pm0.3\,\mu m$, respectively.

3.2. SEM observation and immunohistochemical localization studies

Fig. 3 shows a SEM image of HeLa cells grown on the PADC film which only has a large pore, while Fig. 4 gives the images for visualizing the localization and expression profile of vinculin, F-actin and nuclei on different focal planes. It was very interesting that multiple directions and layers of HeLa cells were clearly observed to have grown in the pores, with good conditions of cells, including good spreading and normal nuclei (Figs. 3 and 4). In Fig. 4, multiple layers of HeLa cells grew in the pores, with cell 1 at the bottom, cell 2 covering part of the cell cytoplasm and cell 3 covering cell 2 on the top. Fig. 4 shows that the focal adhesion protein vinculin expressed normally and these cells had normal nuclei and cytoskeleton structures (as indicated by F-actin).

Fig. 5 gives the images on the focal planes containing the HeLa cells grown on the PADC film substrate which has both large and small pores. Again, multiple directions and layers of cells are clearly seen in the pores, with good conditions of cells, including good spreading and normal nuclei. Cells 1, 2 and 3 are at the bottom while cells 4 and 5 are covering cell 1 on the top. Furthermore, a protrusion from cell 4 is touching a small pore on the bottom of the large pore.

By comparing Figs. 4 and 5, we did not observe significant differences between the vinculin expression profile in cells grown on the PADC films with or without the additional small pores. This is interesting since our previous results showed that small pores

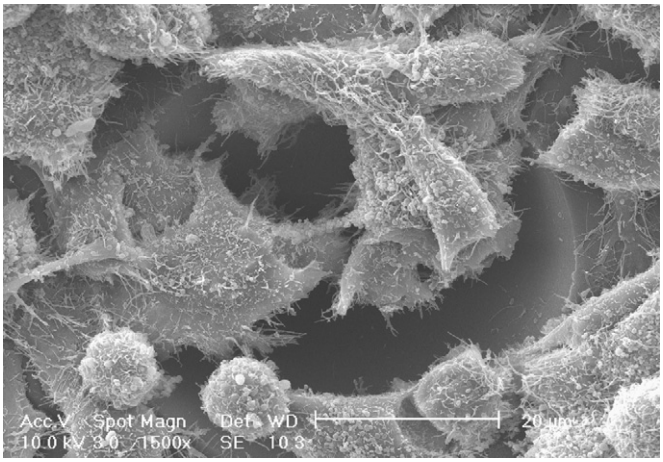

Fig. 3. Representative SEM image of cells grown in a pore. Magnification=1500 ×. Bar=20 μm.

could enhance vinculin expression [23]. The presence of the large pores and/or the enhanced biocompatibility of the substrate in the present experiments might be the reasons. However, from Fig. 5, one can observe that the protrusions of cells are still confined by the small pores, which was also observed in the 2D environment [23].

4. Discussion

Cell–cell and cell–matrix interactions are considerably reduced in the 2D monolayered HeLa cell culture on a flat PADC film substrate, which is characteristic of traditional *in vitro* experiments. Such constraints considerably limit the capability of the cells to recapitulate the suitable level of *in vivo* cellular responses [26]. Cells in the body have multiple of directions with their specific functions, and the direction can affect their potential movement and interactions with the surrounding tissues and cells [27]. For the cells growing within the large spherical pores, as shown in Figs. 3–5, we can see that the cell nuclei are covering one another to large extents. The bottom layer of cells was inside the pores and the cells on top of them spread from the flat area of the substrate into the pore area, covering the cells. Multiple directions and layers of cells were observed in the pores, with good spreading, normal nuclei, normal cytoskeleton structure and cell membrane. The proposed 3D cell culture systems enabled cells to grow in various angles and thus allowed multiple direction of movement. This will better mimic the *in vivo* conditions and provide a better platform for further *in vitro* radiation studies. Such observations were different from the 2D case on Petri dishes or flasks where the cells were too confluent, for which multiple layers could also occur but the cells would then be stressed and tightly packed with round shapes.

According to Zhao et al. [28,29], the average volume and surface-to-volume ratio of a Hela cell were estimated as $2600\,\mu m^3$ [28] and $0.48\pm0.1\,\mu m^{-1}$ [29], respectively. Therefore, the surface area of a Hela cell can be calculated as $1248\pm260\,\mu m^2$. While comparing the data with the pore dimensions (see Section 3.1), it can be found that the surface area and the volume of a single pore were about 2.4 and 8.6 times those of the average cell area and volume, respectively. Therefore, at least 2 cells inside a pore can spread healthily. As the pore provides a base surface area which can accommodate ~2.4 cells and a volume which can accommodate ~8.6 cells, more than one layer of cells can be comfortably accommodated.

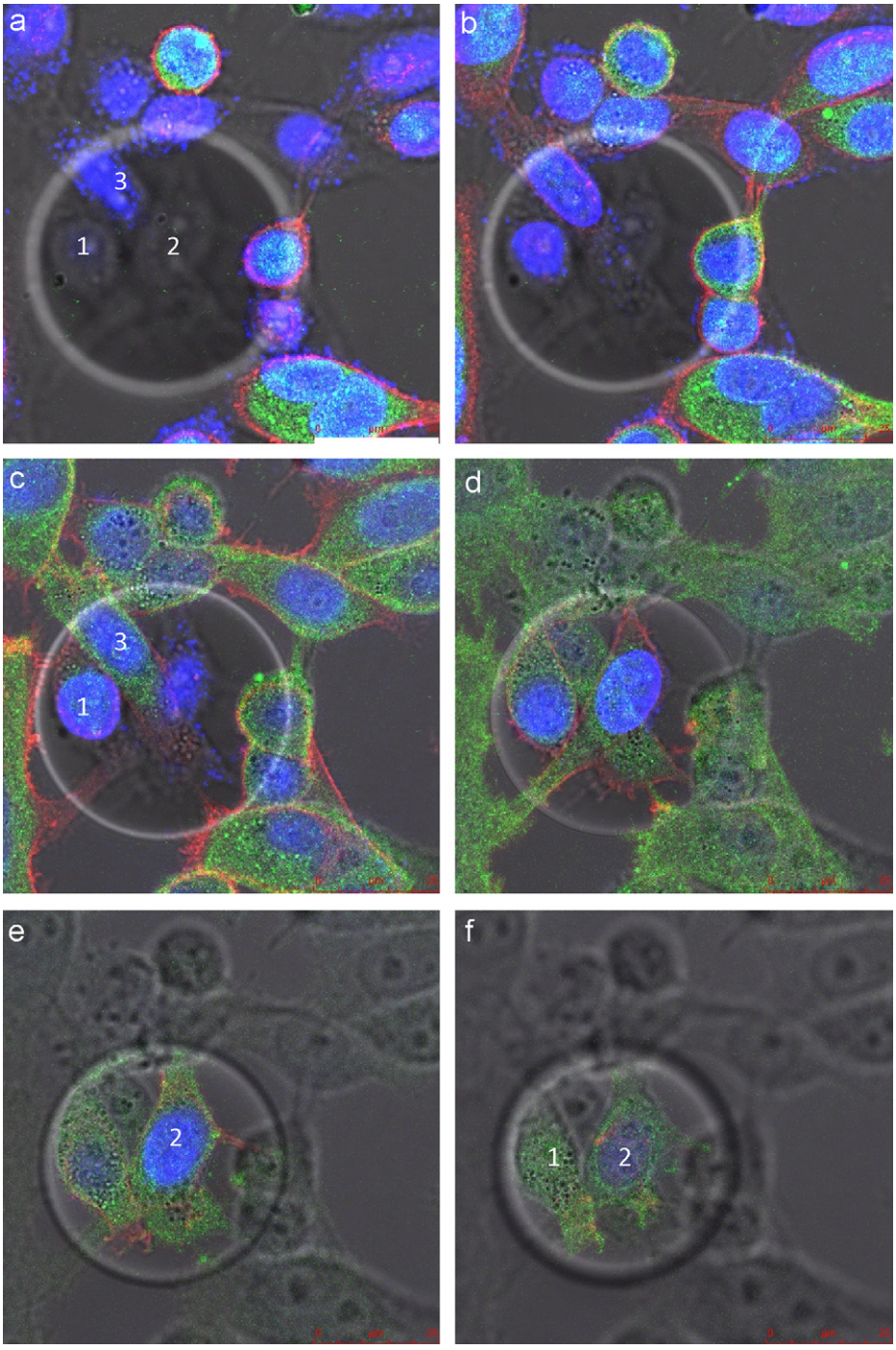

Fig. 4. Representative images showing the spatial expression of vinculin (green), F-actin (red) and nuclei (blue) on HeLa cells obtained using the confocal microscope in different focal planes (4 μm between each plane), in the superposition of vinculin, F-actin, nuclei and transmission mode optical images. Bar=25 μm. From (a) to (f): the focal plane is getting deeper. (For interpretation of the references to colour in this figure legend, the reader is referred to the web version of this article.)

The size of the pores is very important for the design of 3D cell-culture substrates. If the pore size is too large, the curvature will be too small and the pores will resemble a flat dish and might not be able to give enough support to the cells to form more than one layer. On the contrary, if the pore size is too small, the pores will be too small and cannot hold more than one cell. An ideal pore should provide space for spreading of 2 to 3 cells and at the same time provide a suitably included wall to support overlapping of cells. The choice of 30 h etching using aqueous NaOH of the tracks generated by 5 MeV alpha particles in the present work formed pores which could accommodate 2 to 3 cells on the pore bottom (with some cells extending to areas outside the pores or covering other cells), while some more cells supported by the pore wall could stack on the cells on the bottom, so that multiple layers occur.

In conclusion, the large pores provided an environment in which multiple directions and multiple layers of cells could occur and at the same time the cells were not too tight and had good spreading. As such, the biocompatibility was enhanced through the introduction of the micrometer sized pores. The cell–cell and cell–matrix interactions were considerably increased in the 3D environment generated on these specially treated PADC films. Such 3D cell culture substrates enjoyed the convenience in using

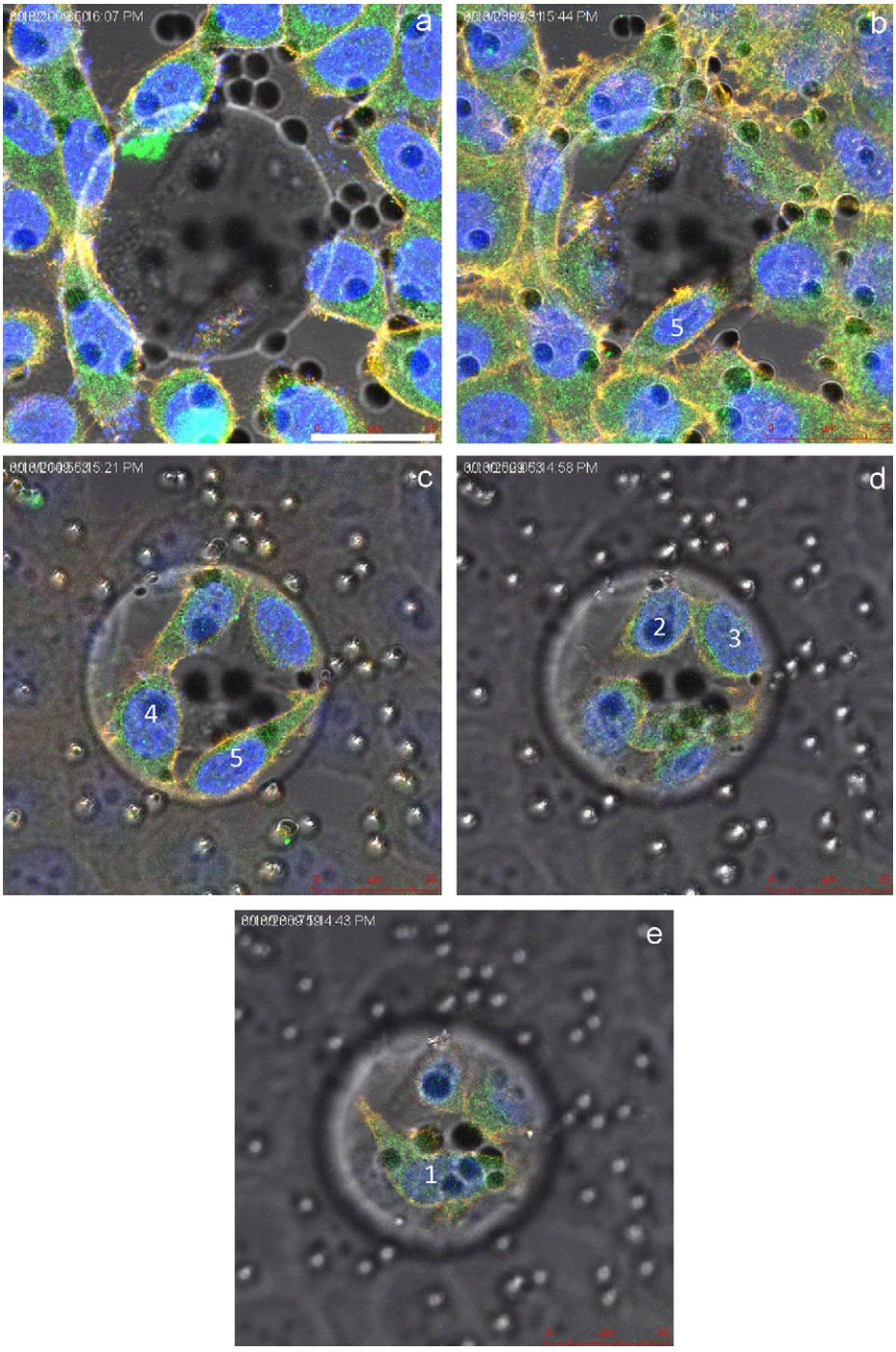

Fig. 5. Representative images showing the spatial expression of vinculin (green), F-actin (red) and nuclei (blue) on HeLa cells obtained using the confocal microscope in different focal planes (4 μm between each plane) in the superposition of vinculin, F-actin, nuclei and transmission mode optical images. Bar=25 μm. From (a) to (e): the focal plane is getting deeper. (For interpretation of the references to colour in this figure legend, the reader is referred to the web version of this article.)

traditional 2D cell culture substrates and at the same time could be used to mimic *in vivo* environments. Vinculin, the cell adhesion and membrane protrusion protein, was used as an indicator of cytoskeletonal reorganization on the substrate and localization of vinculin was used to demonstrate the presence of focal adhesions. The results showed that its expression was about the same while comparing the cells grown within or outside the large pores.

Through small conical pores on a PADC substrate, our previous studies [23] demonstrated for 2D environments that vinculin expression was enhanced and that protrusions from the cells were contained by the pores. By examining Figs. 3 and 4, we could also observe that the membrane edges of HeLa cells tended to be in contact with the small pores, which was consistent with the results for the 2D case [23]. This could again be explained by inhibition of membrane protrusion at the small pores.

In fact, this method has a whole range of flexibilities in generating pores with different characteristics. If another cell type is used, and if the cell volume and area are known, the pore dimensions can be designed according to Eqs. (1)–(3), which can then be achieved by varying the etching conditions, or the energy

of the alpha particles or both. On the other hand, for the additional small pores, the pore density can be simply controlled by the alpha-particle irradiation time while the pore-opening diameter can be controlled by the etching duration. The track-etch pores employed in the current study were conical ($4.8 \pm 0.1\,\mu m$ diameter and $6.6 \pm 0.3\,\mu m$ depth) and spherical ($50.7 \pm 0.4\,\mu m$ diameter and $18.8 \pm 0.2\,\mu m$ depth), but other pore profiles such as conical at the top and spherical at the bottom are also possible by controlling the alpha-particle incident energy and the etching duration. Profiles can be conveniently designed with the help of the TRACK_TEST computer program [17]. The pores making different angles with the substrate surface can be generated by varying the incident angles of the alpha particles. In these cases, the opening will become elliptical or egg-shaped depending on the etching duration. Combinations of pores described above can also be conveniently introduced to the substrate surface. Therefore, in this paper, we just gave one of the examples in mimicking 3D models (spherical shape large pores with/without small conical pores); many more different kinds of models (pores) can be introduced in the future. For radiobiological experiments on PADC films with a thickness of about $20\,\mu m$, this kind of 3D structure will be preferred.

5. Conclusions

A novel, simple and comparatively cost effective process has been developed to fabricate 3D cell-culture substrates through introduction of micrometer-size pores on PADC films. It was very interesting to observe that the cells grown in the pores formed multiple directions and layers, with good spreading, normal nuclei and cell membrane. Expression of the focal adhesion protein vinculin was about the same in the cells grown within or outside the large pores. The HeLa cells grown on the 3D PADC film substrates tended to have their cell membrane edges contained by the small pores. The use of micrometer-size pores in fabricating 3D cell-culture substrates has a whole range of flexibilities with different pore characteristics with the help of computer simulations.

Acknowledgement

We acknowledge the help from W.L. Chiang for assistance with SEM analyzes.

References

[1] C.D. Roskelley, M.J. Bissell, Biochem. Cell Biol. 73 (1995) 391.
[2] K.L. Schmeichel, M.J. Bissell, J. Cell Sci. 116 (2003) 2377.
[3] E. Cukierman, R. Pankov, D.R. Stevens, K.M. Yamada, Science 294 (2001) 1708.
[4] T. Sun, S. Jackson, J.W. Haycock, S. MacNeil, J. Biotechnol. 122 (2006) 372.
[5] V.M. Weaver, O.W. Petersen, F. Wang, C.A. Larabell, P. Briand, C. Damsky, M.J. Bissell, J. Cell Biol. 137 (1997) 231.
[6] F. Wang, V.M. Weaver, O.W. Petersen, C.A. Larabell, S. Dedhar, P. Briand, R. Lupu, M.J. Bissell, Proc. Natl. Acad. Sci. USA 95 (1998) 14821.
[7] R.M. Hoffman, Cancer Cells 3 (1991) 86.
[8] E.M. Lawler, F.R. Miller, G.H. Heppner, In Vitro 19 (1983) 600.
[9] B.E. Miller, F.R. Miller, G.H. Heppner, Cancer Res. 45 (1985) 4200.
[10] S. Levenberg, N.F. Huang, E. Lavik, A.B. Rogers, J. Itskovitz-Eldor, R. Langer, Proc. Natl. Acad. Sci. USA 100 (2003) 12741.
[11] M.W. Hayman, K.H. Smith, N.R. Cameron, S.A. Przyborski, Biochem. Biophys. Res. Commun. 314 (2004) 483.
[12] W. Tan, T.A. Desai, J. Biomed. Mater. Res. A 72 (2005) 146.
[13] G. Mapili, Y. Lu, S. Chen, K. Roy, J. Biomed. Mater. Res. B 75 (2005) 414.
[14] V.I. Chin, P. Taupin, S. Sanga, J. Scheel, F.H. Gage, S.N. Bhatia, Biotechnol. Bioeng. 88 (2004) 399.
[15] A. Abbott, Nature 424 (2003) 870.
[16] K. Bhadriraju, C.S. Chen, Drug Discovery Today 7 (2002) 612.
[17] D. Nikezic, K.N. Yu, Mater. Sci. Eng. R 46 (2004) 51.
[18] W.Y. Li, K.F. Chan, A.K.W. Tse, W.F. Fong, K.N. Yu, Nucl. Instr. and Meth. B 248 (2006) 319.
[19] S. Gaillard, V. Armbruster, M.A. Hill, T. Gharbi, M. Fromm, Radiat. Res. 163 (2005) 343.
[20] K.F. Chan, B.M.F. Lau, D. Nikezic, A.K.W. Tse, W.F. Fong, K.N. Yu, Nucl. Instr. and Meth. B 263 (2007) 290.
[21] B. Baharloo, M. Textor, D.M. Brunette, J. Biomed. Mater. Res. 74A (2005) 12.
[22] C.K.M. Ng, K.F. Chan, W.Y. Li, A.K.W. Tse, W.F. Fong, T. Cheung, K.N. Yu, Radiat. Meas. 43 (Suppl. 1) (2008) 537.
[23] C.K.M. Ng, W.L. Poon, W.Y. Li, T. Cheung, S.H. Cheng, K.N. Yu, Nucl. Instr. and Meth. B 266 (2008) 3247.
[24] J.P.Y. Ho, C.W.Y. Yip, D. Nikezic, K.N. Yu, Radiat. Meas. 36 (2003) 141.
[25] K.F. Chan, F.M.F. Ng, D. Nikezic, K.N. Yu, Nucl. Instr. and Meth. B 263 (2007) 284.
[26] J. Lee, G.D. Lilly, R.C. Doty, P. Podsiadlo, N.A. Kotov, Small 5 (2009) 213.
[27] C.C. Wong, C.M. Wong, E.K. Tung, K. Man, I.O. Ng, Hepatology 49 (2009) 1583.
[28] L. Zhao, C.D. Kroenke, J. Song, D. Piwnica-Worms, J.J.H. Ackerman, J.J. Neil, NMR Biomed. 21 (2008) 159.
[29] L. Zhao, A.L. Sukstanskii, C.D. Kroenke, J. Song, D. Piwnica-Worms, J.J.H. Ackerman, J.J. Neil, Magn. Reson. Med. 59 (2008) 79.